

RSC Advances



This is an *Accepted Manuscript*, which has been through the Royal Society of Chemistry peer review process and has been accepted for publication.

Accepted Manuscripts are published online shortly after acceptance, before technical editing, formatting and proof reading. Using this free service, authors can make their results available to the community, in citable form, before we publish the edited article. This *Accepted Manuscript* will be replaced by the edited, formatted and paginated article as soon as this is available.

You can find more information about *Accepted Manuscripts* in the [Information for Authors](#).

Please note that technical editing may introduce minor changes to the text and/or graphics, which may alter content. The journal's standard [Terms & Conditions](#) and the [Ethical guidelines](#) still apply. In no event shall the Royal Society of Chemistry be held responsible for any errors or omissions in this *Accepted Manuscript* or any consequences arising from the use of any information it contains.

Multiporous open-cell poly(vinyl formal) foams for sound absorption

Bai Xue^{1,2}, Jianguo Deng^{2*}, Junhua Zhang^{1*}

1 The State Key Laboratory of Polymer Materials Engineering, Polymer Research Institute of Sichuan University, Chengdu 610065, China

2 New materials R & D center, Institute of Chemical Material, China Academy of Engineering Physics, Mianyang 621900, China

*Corresponding author. Jianguo Deng, E-mail: d13258430956@126.com. Phone Number: 13258430956

Junhua Zhang, E-mail: zhangjh@scu.edu.cn. Fax number: 86-28-85402465

Abstract: A series of multiporous open-cell poly(vinyl formal) (PVF) foams were obtained by crosslinking poly(vinyl alcohol) (PVA) with different contents of formaldehyde in aqueous solution. Water did not only act as the solvent of PVA, but also as the pore-forming agent during the acetalization process. With the increasing acetalization degree, the multiporous PVF foams gradually separated out from water. And the higher acetalization degree reached, the bigger volume shrinkage was observed. PVF foams with different pore sizes were obtained by changing the formaldehyde dosage. According to the results of FTIR spectra, the intensity ratio of O-H and C-H stretching mode ($\nu_s(\text{O-H})/\nu_s(\text{C-H})$) could reveal the acetalization degrees of PVF foams. The thermal properties and morphologies were investigated by differential scanning calorimetry (DSC), thermogravimetric analysis (TGA), and scanning electron microscope (SEM). The PVF foams could be used as sound absorbing materials because of the open-cell multiporous structures. The sound absorption coefficient (α) of PVF foam largely increased with the decreasing pore size, especially in the frequency range of 800-2500 Hz. And the highest α value of 0.98 was obtained at

2000 Hz for PVF-3.0.

1. Introduction

Poly(vinyl alcohol) (PVA) is one of the synthetic, water-soluble and environmentally friendly polymers, which has a number of applications in the areas of drug delivery, membrane, colloid stabilizer, adhesives, and sizing agent in textile industries.¹⁻⁵ Chemical modification of PVA could be easily achieved because of its high active hydroxyl functional groups which are available for further reactions.⁶ PVA crosslinked with many monomers, such as formaldehyde,⁷⁻⁹ glutaraldehyde,^{6,10} acrolein,¹¹ fumaric acid,¹² alkoxy silanes¹³⁻¹⁵ etc, usually has good chemical, thermal, and mechanical stability.

Among these crosslinking reactions, PVA crosslinked with formaldehyde is identified as poly(vinyl formal) (PVF). PVF is a copolymer of unreacted vinyl alcohol and formal rings. Therefore, the properties and applications of PVF mainly depend on the relative content of functional groups of the reactants and the acetalization degree. PVF with lower acetalization degree (the molar ratio of formaldehyde to hydroxyl is less than 0.1) is still water-soluble, which can be used as adhesive.¹⁶ With the increasing formaldehyde dosage, PVF gels can be prepared and even three-dimensional solid PVF may be obtained. In order to get the three-dimensional PVF, much excessive formaldehyde is introduced to increase the acetalization degree. Flory^{17, 18} reported that if only adjacent intramolecular hydroxyl groups participated in the acetalization, the acetalization degree was 86.46 mol% for 1, 3-glycol structure and 81.6 mol% for 1, 2-glycol structure.

If a suitable pore-forming agent, such as corn starch, surfactants, or the reagents^{19,20} that can

produce gas during the reaction process (e.g. calcium carbonate ²¹), is introduced in the acetalization process, multiporous open-cell PVF foams can be prepared. Previous researches have ever confirmed that the foams are appropriate for pressure-driven membranes designed for wastewater treatment, cells and tissue cultivation etc. ²² However, the pore size of the PVF foam prepared by this method is usually larger than 25 μm . ²¹ It seems to be difficult to obtain smaller pore size by introducing additional pore-forming agents. During the PVA acetalization process, we find that PVF foams gradually separate out from the homogeneous solution; the volumes of PVF foams gradually shrink with the increasing acetalization degree. That is to say, water is continuously excluded during the acetalization process. It gives us a hint that the solvent water may be used as the pore-forming agent to obtain multiporous structure without any other additional pore-forming agents. And it can be expected to obtain different pore sizes by changing the formaldehyde amount.

In addition, as the undesirable and hazardous noise is becoming serious and the demand for a high-class residential environment is increasing, the lightweight, thin, and low-cost substitutes of wood-based materials that are able to absorb sound in wide frequency regions have attracted a considerable research interests. ²³ Polymers have been widely utilized as sound-absorbing materials in the areas of buildings, machinery enclosures, duct liners, etc. ²⁴ We surprisedly find that multiporous PVF foams with open-cell structures have great potential in the application of sound-absorbent materials.

According to the train of thought, PVF foams with relatively small pore sizes (2-10 μm) were prepared by introducing different amount (the molar ratio of formaldehyde to hydroxyl groups

was ranging from 0.5 to 3.0) of formaldehyde into 10 wt% PVA solution. This in-site foaming method by using water as the pore-forming agent is environmental-friendly and quite simple. The open-cell foams were further evaluated as their potential use in sound absorption. To the best of our knowledge, multiporous PVF foams using as novel sound absorbing materials are rarely reported. It is believed in this research that the sound absorption coefficient of PVF foam largely increases with the decreasing pore size.

2. Experimental

2.1 Materials

Poly(vinyl alcohol) (PVA) with a polymerization degree of ca. 1700 and a saponification degree of 99 mol% was purchased from Sichuan Vinylon Co. (China). Formaldehyde (38 wt% aqueous solution) and sulfuric acid were obtained as analytically pure reagents from Chengdu Kelong Chemical Reagent Co., Ltd (China). All the starting materials were used without further purification. Deionized water was prepared in the lab.

2.2 Preparation of PVF foams

PVA (10 g) was dissolved in distilled water (90 g) at 90 °C for 6 h to obtain 10 wt% aqueous solution and then cooled to room temperature. 60 g PVA solution was added to a 250 ml three-necked round-bottomed flask with a mechanical stirrer. And a certain amount of formaldehyde and sulfuric acid (as shown in Table 1) were added into the solution with continuous agitation to make the homogeneous solution. Then the homogeneous solution was transferred to a mold and reacted at 80 °C for 5h. The product was washed with large amount of distilled water to remove formaldehyde and sulfuric acid. After that, the product was cut into desired shape and then

freeze-dried for 48 h. So a series of PVF foams containing PVF-0.5 (0.5 is the molar ratio of formaldehyde to hydroxyl groups of PVA), PVF-1.0, PVF-1.5, PVF-2.0, PVF-2.5, and PVF-3.0 were prepared.

2.3 Measurements

2.3.1 FTIR analysis

Fourier transform infrared (FTIR) analysis of PVF foam was carried out with a Thermo Electron Corporation Nicolet 6700 FTIR spectrometer. A total accumulation of 24 scans and a resolution of 4 cm^{-1} were adequate to obtain high signal-to-noise spectra in the range of $4000\text{-}500\text{ cm}^{-1}$.

2.3.2 Foam structure characterizations

The foam density was geometrically measured according to ISO 845:2006.²⁹ The result was calculated with the help of the following equation:

$$\rho = m/v \quad (1)$$

Where ρ stands for the apparent density, m and v denote the mass and volume of the sample, respectively.

The morphology of PVF foam was observed by a scanning electron microscope (SEM; JEOL, JSM-5900, Japan) with an acceleration voltage of 15 kV. The samples were cryogenically fractured in liquid nitrogen. All the fractured surfaces were coated with gold to enhance the image resolution.

The equilibrium swelling of the foam was investigated by a conventional gravimetric

procedure. In brief, dry foam samples were weighed on an analytical balance, and then immersed into distilled water at ambient temperature. The samples were taken out at predetermined time intervals, gently wiped with filter papers to remove excess distilled water and weighed again.

2.3.3 Differential Scanning Calorimetry

A differential scanning calorimeter (DSC; DSC-204, Netzsch, Germany) was applied to study the thermal properties of PVF foams. The temperature of the DSC apparatus and the heat of fusion were calibrated with indium. Experiments were performed with 7-8 mg samples in aluminum sample pans under a nitrogen flow of 40 ml/min. Firstly, the samples were quickly heated from 30 °C to 240 °C and held at 240 °C for 5 min to eliminate the previous thermal history. And then the samples were cooled at a rate of 10 °C/min to 30 °C. Subsequently, they were scanned from 30 °C to 240 °C at a heating rate of 10 °C/min.

2.3.4 Thermogravimetric Analysis

Thermogravimetric analysis (TGA) was conducted on a TGA analyzer (TA Q600, America). 5-10 mg samples were heated from 30 °C to 800 °C at a heating rate of 10 °C/min, under a nitrogen atmosphere with a purge rate of 60 ml/min. The residual weights of the samples were recorded in the heating process.

2.3.5 Sound absorption properties

Sound absorption properties of the foams were assessed by the impedance tube method, (BSWA Technology Co., China). Diameter of the sample for the measurement is around 60 mm. All the values were obtained as the average of at least three times at ambient temperature.

The schematic of testing sound absorption coefficient is shown in Fig. 1. A loudspeaker as a sound source was settled on the one side of the tube and the specimen was placed on the opposite side.

3. Results and discussion

3.1 FTIR analysis

FTIR spectra of PVA and PVF-0.5 are shown in Fig. 2. In the FTIR spectrum of PVA, a broad band is observed in the range of 3640-3000 cm^{-1} which corresponds to the O-H stretching mode, including free hydroxyl groups and hydrogen bonds.²⁵ However, the hydroxyl stretching band of PVF-0.5 transfers to higher wavenumber (from 3357 to 3463 cm^{-1}) and the intensity relatively decreases, which is ascribed to the decreasing hydroxyl groups with the acetalization. The O-H bending vibration is observed at around 1640 cm^{-1} in both spectra of PVA and PVF. The band in the range of 2950-2900 cm^{-1} is considered as the asymmetric and symmetric stretching modes of $-\text{CH}_2$ groups. In the FTIR spectrum of PVF-0.5, these bands attributed to $-\text{CH}_2$ stretching mode split into 2930, 2857, 2776, and 2680 cm^{-1} because of the introduction of $-\text{O}-\text{CH}_2-\text{O}-$ with the acetalization reaction.²⁶ And new bands also appear at 1475, 1428, 1400, 1360 cm^{-1} which are assigned to the C-H bending modes of PVF.²⁶ The intensities of these PVF-0.5 bands are largely increased with the acetalization because more $-\text{CH}_2-$ groups are introduced into polymer chains. The band centered at 1094 cm^{-1} represents the C-O stretching vibration of PVA. The bands at 1184, 1138, 1065, and 1010 cm^{-1} in the FTIR spectrum of PVF-0.5 relate to C-O-C-O-C stretching vibrations.

FTIR spectra of PVF foams obtained from crosslinking PVA with different contents of

formaldehyde are shown in Fig. 3. It is clearly seen that the characteristic peaks of PVF as described above are all observed in the spectra of Fig. 3. It is noticed that $\nu(\text{O-H})$ and $\nu(\text{C-H})$ bands will change with the increasing formaldehyde amount. So the intensity ratio of O-H and C-H stretching mode ($\nu_s(\text{O-H})/\nu_s(\text{C-H})$) can be applied to determine the acetalization degree of PVF foam.

The influence of formaldehyde dosage on the intensity ratio ($I_{\nu}(\text{O-H})/I_{\nu}(\text{C-H})$) is illustrated in Fig. 4. It can be easily found that the value of $I_{\nu}(\text{O-H})/I_{\nu}(\text{C-H})$ decreases with the increasing formaldehyde dosage. The most probable reason is that the hydroxyl groups gradually react to introduce increasing methylene groups during acetalization process. There is an obvious inflection point at the molar ratio of 1.5. When the molar ratio of formaldehyde to hydroxyl groups is less than 1.5, the $I_{\nu}(\text{O-H})/I_{\nu}(\text{C-H})$ decreases quickly from 9.4 of pure PVA to 1.45; at the molar ratio greater than 1.5, the $I_{\nu}(\text{O-H})/I_{\nu}(\text{C-H})$ is insensitive to the molar ratio. This demonstrates that the acetalization degree of PVF increases quickly with the incremental formaldehyde dosage at lower molar ratio of formaldehyde to hydroxyl groups. However, the acetalization degree is hardly further improved by increasing the formaldehyde dosage after the molar ratio higher than 1.5.

3.2 Foam structure characterization

The SEM images of PVF foams are shown in Fig. 5. The pore sizes and shapes of PVF foams are rather different. The pores present elliptical shapes because distortions of the foam structures could occur during the drying process.^{27, 28}

The pore size and cell density (N_0) of PVF foam were statistically obtained with the software Image-Pro Plus 6.0 from the SEM images. The cell density was determined using the equation as

follows:

$$N_0 = \left(\frac{n}{A}\right)^{3/2} \times \frac{\rho}{\rho_f} \quad (2)$$

Where n stands for the number of cells in the SEM micrograph, A is the area of the image with a value of $6.67 \times 10^{-10} \text{ m}^2$, ρ with a value of $1.20 \times 10^3 \text{ kg/m}^3$ is the density of PVF resin and ρ_f is the density of PVF foam.^{29, 30}

The porosity of the foam was calculated as follows:³¹

$$P = \frac{(G_2 - G_1)\rho_l}{(G_2 - G_3 + G_4)\rho_{sa}} \quad (3)$$

Where P is the porosity of the foam, G_1 is the weight of the dry PVF foam, G_2 is the weight of the PVF foam soaked for 24, G_3 is the total weight of the soaked foam, trays and weight in the water, G_4 with a value of 3.65 N stands for the weight of the trays and weight in the water, ρ_l is the density of water with a value of $1.00 \times 10^3 \text{ kg/m}^3$, and ρ_{sa} is the density of the water soaking PVF foam for 24 h.

As shown in Fig. 6a, it is obviously seen that the increase of formaldehyde dosage leads to the decreasing pore size, which can be explained by an increase of the crosslinked polymer part in the volume unit. More rapid formation of the three-dimensional structure of the polymeric matrix can also cause the decrease of the pore size.^{32, 33} The pore size decreases rapidly from $10.4 \mu\text{m}$ to $2.8 \mu\text{m}$ with the incremental formaldehyde dosage at the molar ratio of formaldehyde to hydroxyl groups less than 1.5; when the molar ratio is higher than 1.5, the pore size decreases relatively slowly from $2.8 \mu\text{m}$ to $1.9 \mu\text{m}$. Moreover, the ratio between the major axis and minor axis also decreases with the increasing formaldehyde amount, which demonstrates that the strength of foam

walls is increased and the ability of maintaining the initial shape is improved.

Fig. 6b shows the mean diameter distributions of the PVF foams with different acetalization degree. It is clearly seen that the size distribution is narrower and the concentrated aperture size decreases with the increasing formaldehyde amount. The number of pores also rapidly increases accompanied with the reduction of pore sizes, which illustrates that the cell density increases as the formaldehyde dosage is increased.

The foam density, cell density, and porosity are summarized in Table 2. What's noticeable is that the density of PVF-0.5 ($1.09 \times 10^3 \text{ kg/m}^3$) is higher than that of water. The foam density decreases with the incremental molar ratio of formaldehyde to hydroxyl. The strength of foam walls is improved and the ability of keeping porous structures is largely enhanced at higher formaldehyde amount. Thus the distortions of the pores during the drying process are largely decreased, which directly results in the decrease of PVF foam density. On the contrary, the porosity of PVF foam increases with the incremental formaldehyde amount.

3.3 Equilibrium swelling study

The equilibrium swelling was calculated with the help of following equation:

$$S = \frac{m_s - m_d}{m_d} \quad (4)$$

Where S is the equilibrium swelling degree of the foam, m_s is the mass of swollen foams, m_d is the mass of dry foam.

As shown in Fig. 5, PVF foams consist of a large number of reach-through pores occupying a considerable part of the volume unit. The reach-through pores are divided by zones of cross-linked

polymer. The swelling of PVF foams is mainly due to the increase of the free-water content which does not participate in hydrogen bonds with polymer chains.³⁴ The water absorbency directly depends on crosslinking density of the PVF foam.³⁵

The effect of the formaldehyde dosage on the swelling of PVF foam is shown in Fig. 7. The equilibrium swelling degrees of PVF foams are listed in Table 2. The results clearly reveal that the swelling degree increases with the incremental formaldehyde dosage. It is the pore size and porosity that mainly influence the swelling degree of PVF foam. At low acetalization degree, the pore may be collapsed (as shown in Fig. 5, PVF-0.5) and the porosity decreases during the drying process. The diffusion of water into the shrunken pores is very difficult, which results in the lower equilibrium swelling degree. The strength of the pore walls increases with the incremental acetalization degree, which is beneficial to maintaining the multiporous structures and increasing the porosity. In addition, the swelling speed also increases with the increasing dosage of formaldehyde. For example, PVF-0.5 reaches the equilibrium swelling at about 110 min, however, the equilibrium swelling of PVF-3.0 only takes 10 min.

3.4 Thermal stability

The reheating and cooling DSC curves of PVA and PVF foams are shown in Fig. 8. For clarity, all DSC scan curves shown here are shifted vertically. From Fig. 8a, it can be observed that PVA exhibits an endothermic peak at about 227 °C, corresponding to the melting temperature of PVA. No endothermic melting peaks are observed in the DSC curves of PVF foams, due to the formation of crosslinked networks between PVA and formaldehyde. The glass-transition temperature (T_g) of PVA is only 71.5 °C, however, the T_g of PVF drastically increases to around

120 °C, because crosslinked networks limit the mobility of the PVA chains. This implies that the PVF foams obtained in this study are characterized by high thermostability even heating to more than 100 °C.³⁶⁻³⁸ As shown in Fig. 8b, a single exothermic peak at about 182 °C appears in the DSC cooling curve of PVA. No exothermic peaks could be observed in the DSC cooling curves of PVF foams, which is consistent with the reheating DSC curves. The glass-transition temperatures obtained from cooling curves have no clear difference with those from reheating curves.

The TGA thermograms for PVA and PVF foams are shown in Fig. 9. Not all the thermograms are shown here to gain a clear visualization. The weight loss of PVA below 150 °C is mainly due to the evaporation of free water molecules in PVA owing to its hydrophilic property.³⁹ The weight loss of PVF foam below 150 °C is much lower than that of PVA, which is attributed to the decreasing hydrophilic property with the acetalization. As shown in TGA curves, it is clearly seen that the thermal degradation of PVF is in three steps. The initial decomposition of PVF is due to the cleavage of the formal ring and the removal of water from neighbouring pairs of unreacted hydroxyl groups.⁴⁰ The threshold temperatures for weight loss of PVF-1.0, PVF-2.0, and PVF-3.0 are 192.6 °C, 181.1 °C, and 166.4 °C, and correspondingly the first peak temperatures for main weight loss are 210.9 °C, 217.4 °C, and 216.7 °C. As there are no formal rings in PVA chains, the first peak temperature for main weight loss of PVA transfers to 262.4 °C, corresponding to the removal of water from neighbouring pairs of hydroxyl groups. The second-stage degradation is due to the removal of CO, CO₂, hydrocarbons, etc. from the PVF foam and the third-stage degradation of PVF is ascribed to the production of carbon.⁴¹

3.5 Acoustical property

As shown in Fig. 1, the sound pressures at two microphone locations (p_1, p_2) were measured and the values are shown in equations (5) and (6):

$$p_1 = \check{p}_I e^{jk_0 x_1} + \check{p}_R e^{-jk_0 x_1} \quad (5)$$

And

$$p_2 = \check{p}_I e^{jk_0 x_2} + \check{p}_R e^{-jk_0 x_2} \quad (6)$$

Where \check{p}_I is the amplitude of normal incidence sound pressure and \check{p}_R is the amplitude of normal reflection sound pressure. k_0 stands for the wave number. x_1 and x_2 denote the distances between the two microphones and the sample, respectively.

The sound absorption coefficient (α) could be evaluated according to the equation (7)

$$\alpha = 1 - |\gamma|^2 \quad (7)$$

Where γ is the normal incidence sound pressure reflection factor.

And
$$\check{p}_R = \gamma \check{p}_I \quad (8)$$

Relating equations (5) to (8), the equation (9) could be obtained:

$$\alpha = 1 - \left| \frac{p_2 e^{jk_0 x_1} - p_1 e^{jk_0 x_2}}{p_1 e^{-jk_0 x_2} - p_2 e^{-jk_0 x_1}} \right|^2 \quad (9)$$

When the incident sound wave (E_i) transmits through the surface of the sample, it will divide into three portions: absorption sound wave (E_a), reflection sound wave (E_r) and transmitting sound wave (E_t), as shown in the equation (10).

$$E_i = E_t + E_r + E_a \quad (10)$$

The normally incident sound absorption coefficient (α) is obtained by the equation (11):

$$\alpha = \frac{E_a}{E_i} \quad (11)$$

Sound absorption coefficients of the PVF foams as the function of frequency are shown in Fig. 10a. In general, sound absorption coefficient increases with the incremental frequency, according to the Stokes-Kirchhoff formula. And the peak value of α is observed at the resonance frequency.³⁷ For the PVF foam, the sound absorption coefficient is very low (less than 0.3) in the frequency range lower than 800 Hz. And the sound absorption coefficient fluctuates violently in this frequency range. In the higher frequency range, the sound absorption coefficient rapidly increases with the increasing frequency. The absorption peak of the sample is observed at the frequency of 2000 Hz which is ascribed to the specific characteristic of PVF foam.

For a quantitative comparison, the average coefficients of sound absorption ($\bar{\alpha}$) for these materials can be calculated by using the following equation (12):⁴²

$$\bar{\alpha} = \frac{\int_{F_1}^{F_2} \alpha(f) df}{F_2 - F_1} \quad (12)$$

Where F_1 and F_2 are the starting and ending frequency, respectively. The mean sound absorption coefficient as a function of the molar ratio of formaldehyde to hydroxyl is shown in Fig. 10b. The average sound absorption coefficient ($\bar{\alpha}$) obviously increases with the increasing formaldehyde amount and the highest $\bar{\alpha}$ value of 0.54 is obtained for PVF-3.0. The most probable reason is that the pore size decreases with the incremental acetalization degree, however, the porosity of the PVF foam increases as the dosage of formaldehyde is increased. The material with highly porous structure exhibits a good ability of normally incident sound absorption.^{24, 43} When the incident sound wave passes through the porous material, the vibration of air in the pore and the mechanical friction between the non-rigid pore frame and air will consume large amounts

of energy of the sound wave.⁴⁴⁻⁴⁷

Conclusion

In the present work, PVF foams with excellent sound absorption properties were prepared by crosslinking PVA with different formaldehyde dosage in the presence of sulfuric acid catalyst. This in-site foaming method by using water as the pore-forming agent is environmental-friendly and quite simple. The sound absorption coefficient of the PVF foam largely increases with the increasing formaldehyde dosage, especially in the frequency range of 800-2500 Hz. The highest α value of 0.98 is obtained at 2000 Hz for PVF-3.0. According to the results of FTIR analysis, the value of $I_{\nu}(\text{O-H})/I_{\nu}(\text{C-H})$ decreases with the increasing formaldehyde dosage, which demonstrates that the acetalization degree of PVF is increased. However, the $I_{\nu}(\text{O-H})/I_{\nu}(\text{C-H})$ decreases very slowly at the molar ratio of formaldehyde to hydroxyl groups higher than 1.5. According to SEM observations, when the molar ratio is less than 1.5, the pore size of PVF foam decreases rapidly from 10.4 μm to 2.8 μm with the increasing formaldehyde dosage; at the molar ratio higher than 1.5, the pore size decreases very slightly from 2.8 μm to 1.9 μm , which is consistent with the results of FTIR analysis. From the results of DSC, the glass-transition temperature of PVF increases to about 120 °C because the formation of networks in the acetalization process decreases the mobility of PVA chains. TGA shows the thermal degradation of PVF includes three steps: (1) the cleavage of the formal ring and the removal of water from neighbouring pairs of unreacted hydroxyl groups; (2) the removal of carbon dioxide, carbon monoxide, and hydrocarbons; (3) the production of carbon. Moreover, PVF foams with higher acetalization degrees can maintain the multiporous structures well, which is beneficial to the diffusion of water into the foams.

References:

- 1 E. Chiellini, A. Corti, S. D'Antone and R. Solaro, *Prog. Polym. Sci.*, 2003, **28**, 963–1014.
- 2 T. Das, S. Yeasmin, S. Khatua, K. Acharya and A. Bandyopadhyay, *RSC Adv.*, 2015, **5**, 54059-54069.
- 3 J. Li, L. Zhang, J. Gu, Y. Sun and X. Ji, *RSC Adv.*, 2015, **5**, 19859-19864.
- 4 J. Gaume, P. Wong-Wah-Chung, A. Rivaton, S. Therias and J. L. Gardette, *RSC Adv.*, 2011, **1**, 1471-1481.
- 5 H. Z. Zhang, B. L. Liu, R. Luo, Y. Z. Wu, and D. S. Lei, *Polym. Degrad. Stab.*, 2006, **91**, 1740–1746.
- 6 Y. Zhang, P. C. Zhu and D. Edgren, *J. Polym. Res.*, 2010, **17**, 725-730.
- 7 N. Durmaz-Hilmioglu, A. E. Yildirim, A. S. Sakaoglu and S. Tulbentei, *Chem. Eng. Proc.*, 2001, **40**, 263–267.
- 8 B. Han, J. Li, C. Chen, C. Xu and S. R. Wickramasinghe, *Trans. I. Chem. Eng.*, 2003, **81A**, 1385–1392.
- 9 H. N. Chang, *Desalination*, 1982, **42**, 63–77.
- 10 T. Tashima, M. Imai, Y. Kuroda, S. Yagi, and T. Nakagawa, *J. Organic. Chem.*, 1991, **56**, 694–697.
- 11 R. D. Sanderson, E. Immelman, D. Bezuidenhout, E. P. Jacobs and A. J. van Reenen, *Desalination*, 1993, **90**, 15–29.
- 12 Z. Huang, H. M. Guan, W. Tan, X. Qiao and S. Kulprathipanja, *J. Membr. Sci.*, 2006, **276**, 260–271.
- 13 R. Guo, C. Hu, F. Pan, H. Wu and Z. Jiang, *J. Membr. Sci.*, 2006, **281**, 454–462.

- 14 Q. G. Zhang, Q. Liu, Z. Jiang and Y. Chen, *J. Membr. Sci.*, 2007, **287**, 237–245.
- 15 Y. Liu, Y. Su, and J. Lai, *Polymer*, 2004, **45**, 6831–6837.
- 16 S. Amiya, S. Tsuchiya, R. Qian and A. Nakajim, *Pure Appl. Chem.*, 1990, **62**, 2139–2146.
- 17 P. J. Flory, *J. Am. Chem. Soc.*, 1938, **61**, 1518-1521.
- 18 P. J. Flory, *J. Am. Chem. Soc.*, 1950, **72**, 5052-5055.
- 19 N. A. Peppas and S. R. Stauffer, *J. Control. Release*, 1991, **16**, 305–310.
- 20 D. Trimnell, B. S. Shasha and F. H. Otey, *J. Control. Release*, 1985, **1**, 183-190.
- 21 X. Bai, Z. Ye, Y. Li, L. Zhou and L. Yang, *Process Biochem.*, 2010, **45**, 60-66.
- 22 B. Bolto, T. Tran, M. Hoang and Z. Xie, *Prog. Polym. Sci.*, 2009, **34**, 969-981.
- 23 S. Ersoy, and H. Kucuk, *Appl. Acoust.* 2009, **70**, 215-220.
- 24 H. Zhou, B. Li, and G. Huang, *Mater. Lett.*, 2006, **60**, 3451-3456.
- 25 B. J. Holland and J. N. Hay, *Polymer*, 2002, **43**, 2207– 2211.
- 26 P. Chetri and N. N. Dass, *Polymer*, 1997, **38**, 3951-3956.
- 27 F. M. Plieva, M. Karlsson, M. R. Aguilar, D. Gomez, S. Mikhalovsky, I. Y. Galaev and B. Mattiasson, *J. Appl. Polym. Sci.*, 2006, **100**, 1057-1066.
- 28 A. A. Artyukhov, M. I. Shtilman, A. N. Kuskov, A. P. Fomina, D. E. Lisovyv, A. S. Golunova and A. M. Tsatsakis, *J. Polym. Res.*, 2011, **18**, 667-673.
- 29 P. Jia, J. Hu, W. Zhai, Y. Duan, J. Zhang and C. Han, *Ind. Eng. Chem. Res.*, 2015, **54**, 2476-2488.
- 30 D. Jahani, A. Ameli, M. Saniei, W. Ding, C. B. Park and H. E. Naguib, *Macromol. Mater. Eng.*, 2015, **300**, 48-56.
- 31 R. Gong, Q. Xu, Y. Chu, X. Gu, J. Ma, and R. Li, *RSC Adv.*, 2015, **5**, 68003-68013.

- 32 I. Pollers, P. Adriaensens, R. Carleer, D. Vanderzande and J. Gelan, *Macromolecules*, 1996, **29**, 5875-5881.
- 33 A. A. Artyukhov, M. I. Shtilma, A. N. Kuskov, L. I. Pashkova, A. M. Tsatsakis and A. K. Rizos, *J. Non-cryst. Solids*, 2011, **357**, 700-706.
- 34 S. J. Kim, S. J. Park, K. H. An, N. G. Kim and S. I. Kim, *J. Appl. Polym. Sci.*, 2003, **89**, 24-27.
- 35 Y. An, T. Koyama, K. Hanabusa and H. Shirai, *Polymer*, 1995, **36**, 2297-2301.
- 36 J. A. Stammen, S. Williams, D. N. Ku and R. E. Guldberg, *Biomaterials*, 2000, **22**, 799-806.
- 37 S. Eei and H. F. Nag, *Polymer*, 2003, **44**, 1647-1653.
- 38 C. M. Hassan, J. H. Ward and N. A. Peppas, *Polymer*, 2000, **41**, 6729-6739.
- 39 H. Du, T. Zhou, J. Zhang and X. Liu, *Anal. Bioanal. Chem.*, 2010, **397**, 3127-3132.
- 40 H. Aoki and T. Suzuki, *J. Polym. Sci., Polym. Chem.*, 1988, **26**, 31-41.
- 41 D. A. Chatfield, *J. Polym. Sci., Polym. Chem. Ed.*, 1983, **21**, 1681-1691.
- 42 Y. Chen and N. Jiang, *Text. Res. J.*, 2007, **77**, 785-791.
- 43 X. Wang, F. You, F. S. Zhang, J. Li and S. Guo, *J. Appl. Polym. Sci.*, 2011, **122**, 1427-1433.
- 44 H. Zhou, B. Li, G. Huang, and J. He, *J. Sound Vib.*, 2007, **304**, 400-406.
- 45 H. S. Yang, D. J. Kim and H. J. Kim, *Bioresource Technol.*, 2003, **86**, 117-121.
- 46 S. Ersoy and H. Kucuk, *Appl. Acoust.*, 2009, **70**, 215-220.
- 47 S. Jiang, Y. Xu, H. Zhang, C. B. White and X. Yan, *Appl. Acoust.*, 2012, **73**, 243-247.

Figure captions

Fig.1 Schematic diagram of apparatus for measuring sound absorption coefficient.

Fig. 2 FTIR spectra of PVA and PVF-0.5 in the 4000-500 cm^{-1} region.

Fig. 3 FTIR spectra of PVF samples in the region of 4000-500 cm^{-1} .

Fig. 4 $I_{\nu}(\text{O-H})/I_{\nu}(\text{C-H})$ as a function of the molar ratio of formaldehyde to hydroxyl.

Fig. 5 Typical SEM images of cryo-surfaces of the PVF foams.

Fig. 6 (a) Influence of the molar ratio of formaldehyde to hydroxyl on the average pore size, (b)

The pore size distributions of different PVF foams.

Fig. 7 Influence of the molar ratio of formaldehyde to hydroxyl on equilibrium swelling of the

PVF foams.

Fig. 8 (a) DSC reheating curves and (b) cooling curves obtained from PVA and PVF foams.

Fig. 9 TGA thermograms of PVA and PVF foams.

Fig. 10 (a) Sound absorption coefficients of PVF foams as a function of frequency. (b) Effect of

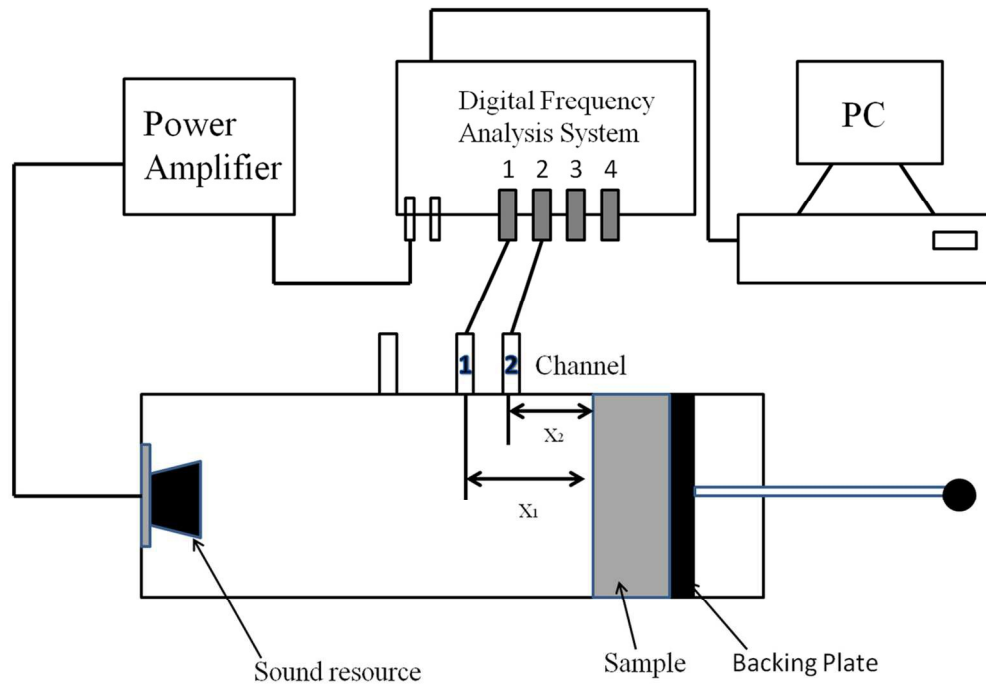
the molar ratio of formaldehyde to hydroxyl on the average sound absorption coefficient ($\bar{\alpha}$).

Table 1 Parameters for the acetalization

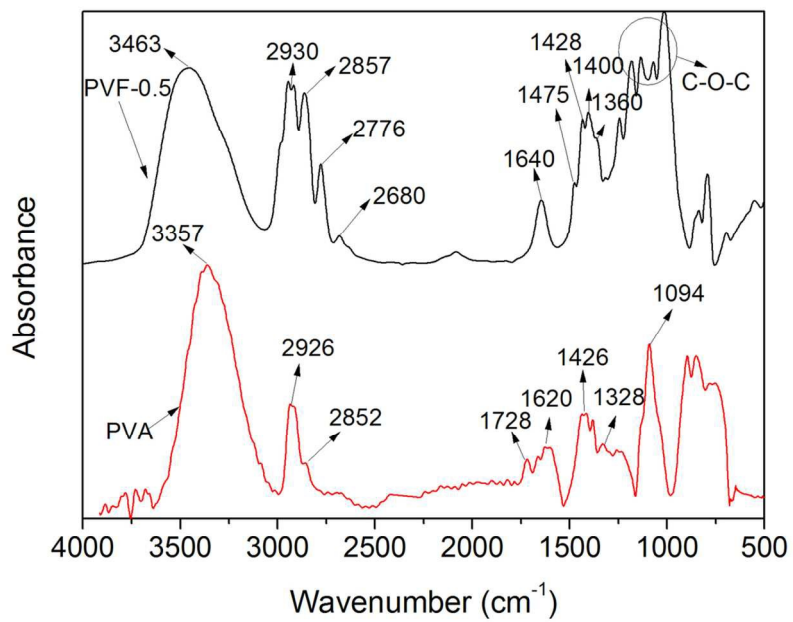
Sample	10% PVA (g)	38% formaldehyde (g)	35% sulfuric acid (g)	Formaldehyde moles per -OH
PVF-0.5	60.00	5.38	6.00	0.5
PVF-1.0	60.00	10.77	6.00	1.0
PVF-1.5	60.00	16.15	6.50	1.5
PVF-2.0	60.00	21.54	7.00	2.0
PVF-2.5	60.00	26.92	7.50	2.5
PVF-3.0	60.00	32.31	8.00	3.0

Table 2 Foam density, cell density, porosity, and equilibrium swelling degree data for different PVF foams

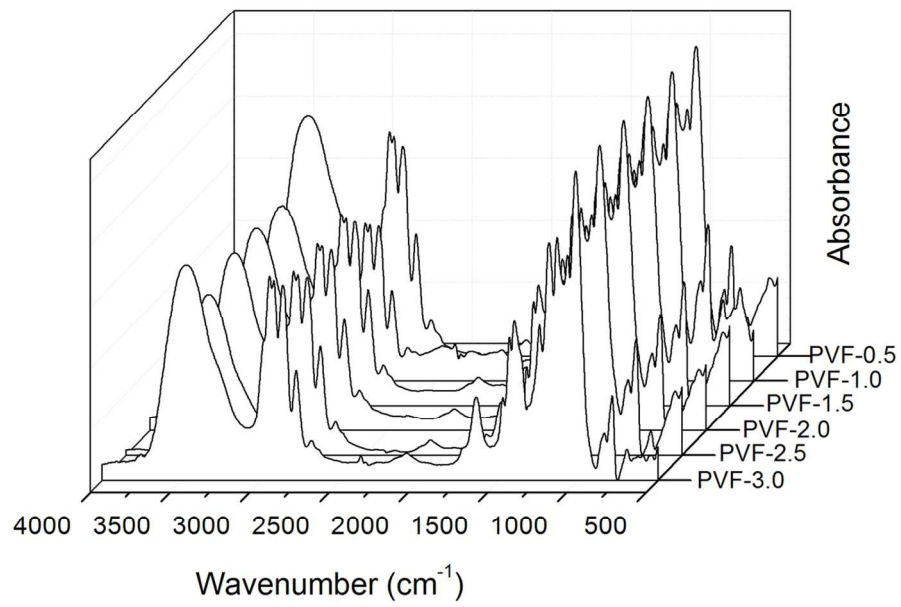
Sample	Foam density (kg/m ³)	Cell density (cells/m ³)	Porosity (%)	Equilibrium swelling degree
PVF-0.5	1090	1.12×10 ¹⁶	54.06	0.59
PVF-1.0	920	9.06×10 ¹⁶	56.61	0.61
PVF-1.5	500	2.06×10 ¹⁷	76.69	1.84
PVF-2.0	460	2.96×10 ¹⁷	82.74	1.92
PVF-2.5	410	7.45×10 ¹⁷	85.44	1.95
PVF-3.0	360	1.84×10 ¹⁸	90.29	2.54



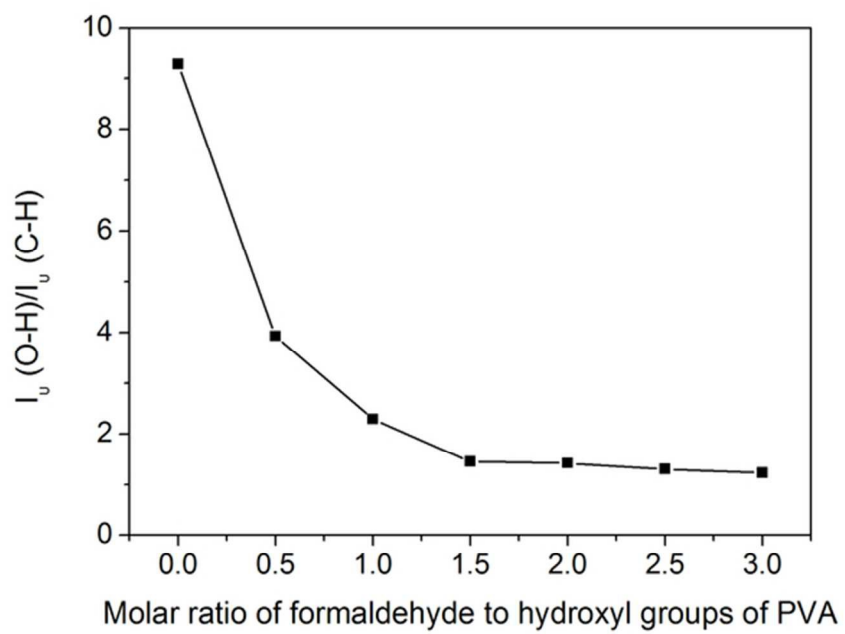
119x83mm (300 x 300 DPI)



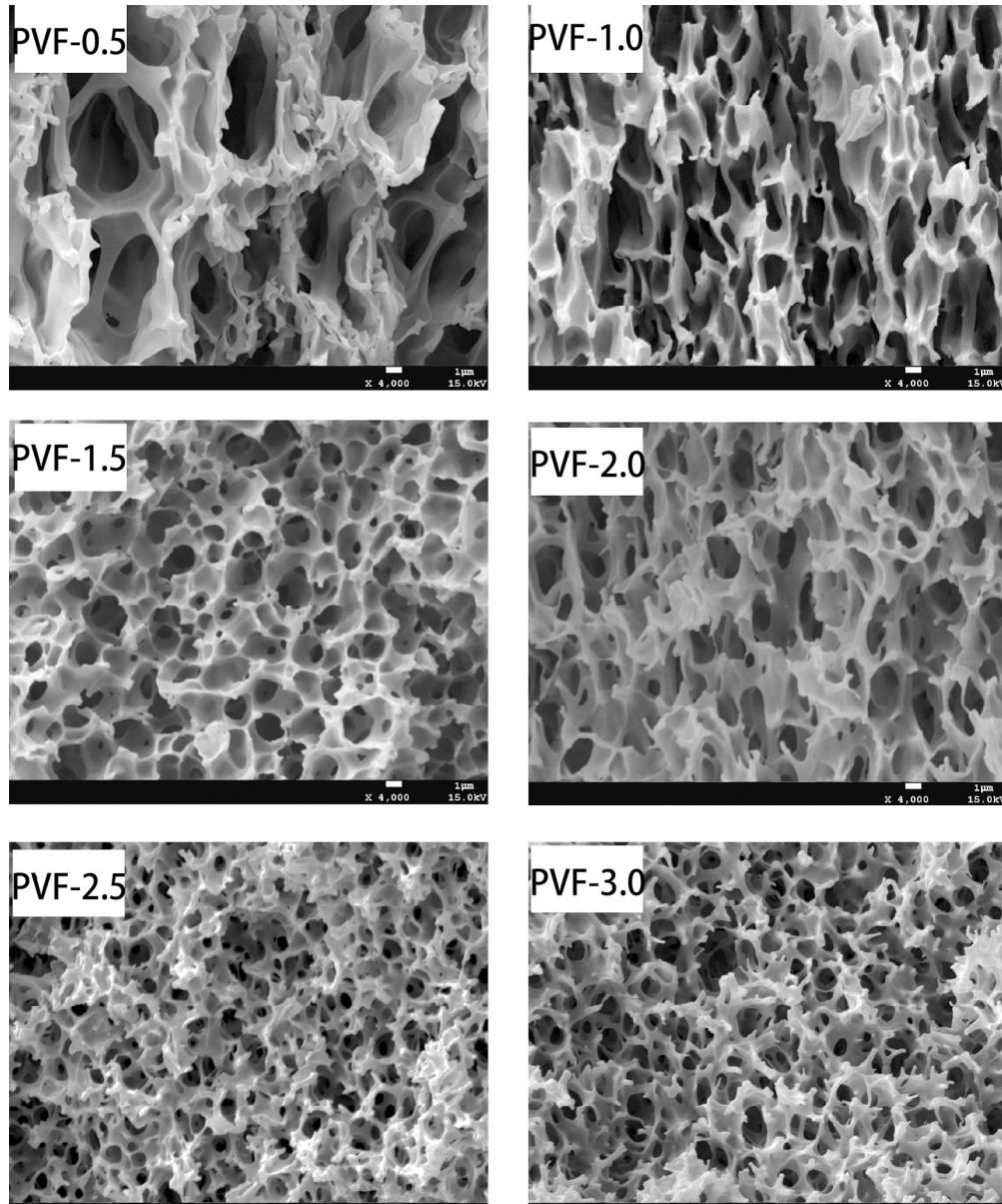
120x85mm (300 x 300 DPI)



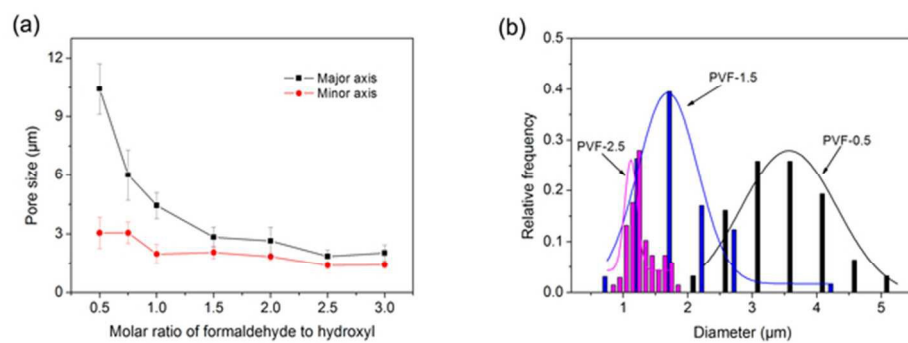
120x85mm (300 x 300 DPI)



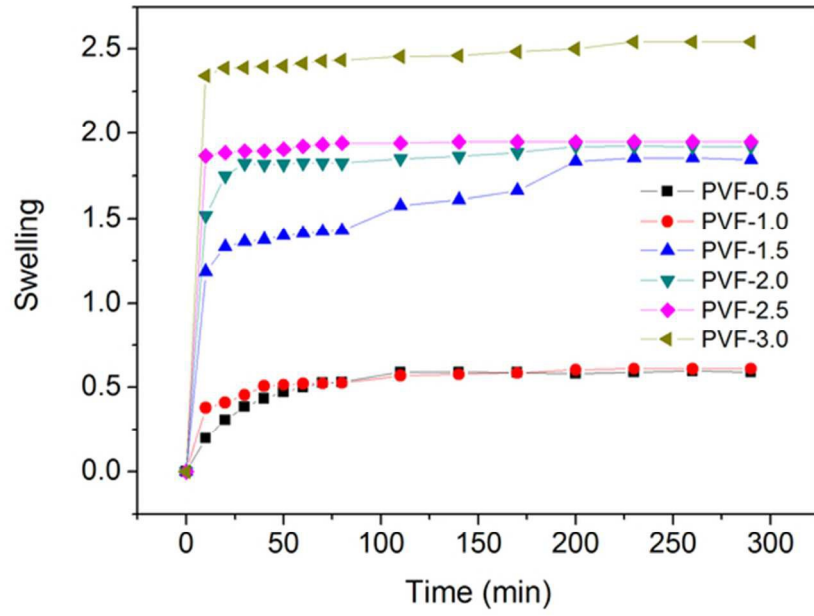
58x41mm (300 x 300 DPI)



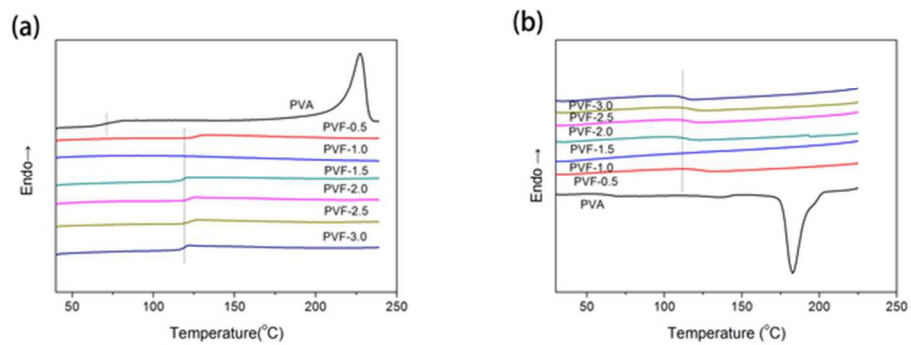
205x246mm (300 x 300 DPI)



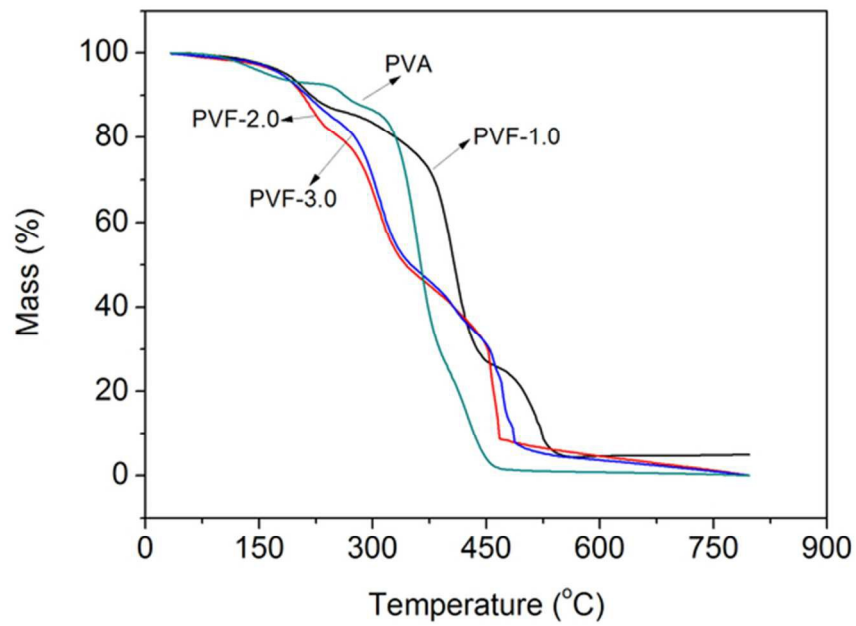
60x21mm (300 x 300 DPI)



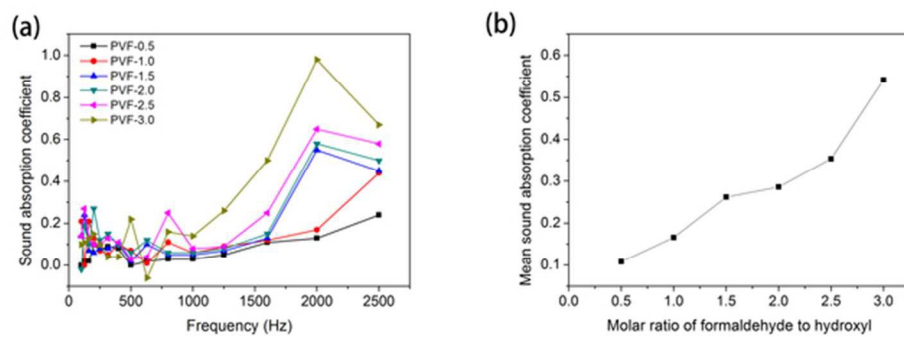
58x41mm (300 x 300 DPI)



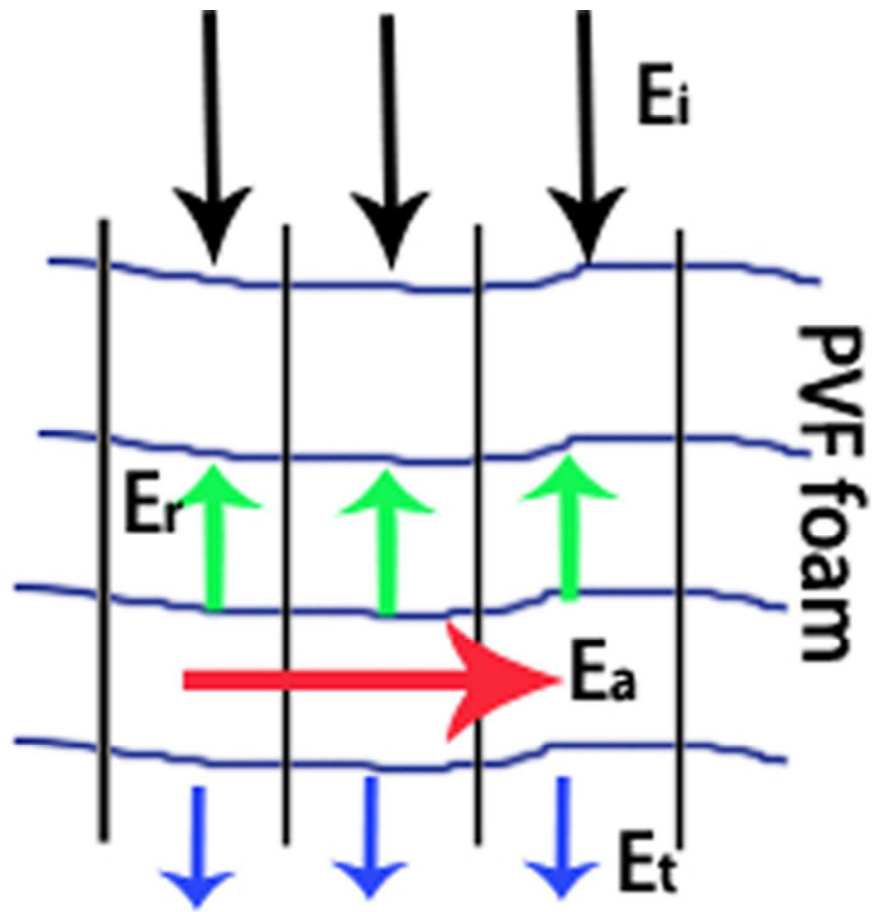
58x20mm (300 x 300 DPI)



58x41mm (300 x 300 DPI)



58x20mm (300 x 300 DPI)



39x39mm (300 x 300 DPI)